

$[\text{H}_3\text{N}(\text{CH}_2)_7\text{NH}_3]_8(\text{CH}_3\text{NH}_3)_2\text{Sn}(\text{IV})\text{Sn}(\text{II})_{12}\text{I}_{46}$ – a mixed-valent hybrid compound with a uniquely templated defect-perovskite structure†‡

Jun Guan, Zhongjia Tang and Arnold M. Guloy*

Received (in Cambridge, UK) 26th July 2004, Accepted 30th September 2004

First published as an Advance Article on the web 19th November 2004

DOI: 10.1039/b411322e

The incorporation of $\text{H}_3\text{N}(\text{CH}_2)_7\text{NH}_3$ with $\text{CH}_3\text{NH}_3\text{SnI}_3$ resulted in the formation of a mixed-valent and semi-conducting ($E_g = 0.84$ eV) organic-based perovskite, $[\text{H}_3\text{N}(\text{CH}_2)_7\text{NH}_3]_8(\text{CH}_3\text{NH}_3)_2\text{Sn}(\text{IV})\text{Sn}(\text{II})_{12}\text{I}_{46}$, with a unique 3D defect-perovskite structure with ordered vacancies at the Sn and I sites.

The electronic delocalization properties of mixed-valent perovskites continue to be of great interest, in part because of their relevance to studies on high- T_c superconductivity¹ as well as catalytic, dielectric, optical, transport and magnetic properties of transition metal perovskites.^{2,3} Introduction of mixed-valency in perovskite compounds is usually accompanied by significant structural distortions, substitutions and/or formation of vacancies and defects within the perovskite framework. The important structural flexibility of perovskites (ABX_3) is partly due to the ability of the B cations to adopt a variety of coordination numbers, and robustness of the B–X network in accommodating vacancies in the cation (A, B) and anion (X) sites.^{3–5} Most defect perovskites (metal oxides and halides) exhibit vacancies at the cation A- ($\text{CN} = 12$) and anion X- (e.g. O, F, Cl, Br, I) sites. However, occurrences of vacancies at the B-sites are rare and have been ascribed to thermodynamic instability of vacancies due to the higher charge and smaller size of the B-cations.⁵

Organic-based metal halide perovskites make up an important class of tunable materials.⁶ In particular, the tunable electronic properties of the hybrid Sn and Pb halides arise from the systematic modular combinations of the organic and inorganic components.⁷ They also exhibit a unique structural flexibility accompanied by a modulation of their electronic properties. This is exemplified by the transition from semiconducting to metallic behavior, with increasing dimensionality, in the different families of layered tin(II) iodide perovskites.^{6,7} Their structures are significantly influenced by the nature and molecular conformations of the organic components, as effectively shown in the families of layered perovskites, and in the polymorphism of α - and β - $(\text{NH}_3(\text{CH}_2)_5\text{NH}_3)\text{SnI}_4$.⁸ The formation of metal defects in organic-based layered perovskites has been templated by organic molecules, albeit in a hybrid Bi(III) iodide.⁹

Efforts to introduce mixed-valency in organic-based Sn halide perovskites have so far been unsuccessful. This important question

relates to the metallic cubic perovskites, CsSnI_3 and $\text{CH}_3\text{NH}_3\text{SnI}_3$, which exhibit high mobilities and low carrier (hole) densities.¹⁰ Yet to date, efforts to increase the carrier (hole) densities by doping (oxidation) have been unsuccessful. Herein we report the synthesis of a mixed-valent organic-based tin halide defect-perovskite, $[\text{H}_3\text{N}(\text{CH}_2)_7\text{NH}_3]_8(\text{CH}_3\text{NH}_3)_2\text{Sn}(\text{IV})\text{Sn}(\text{II})_{12}\text{I}_{46}$ (**1**).

The title compound was prepared by reacting stoichiometric amounts of SnI_2 (0.2 mmol) and the corresponding organic ammonium iodide salts in concentrated HI solution (3 ml). The resulting HI solution was heated to 130 °C and then slowly cooled to room temperature. Formation of very dark-red brick crystals was observed during slow cooling. The crystals were moderately air stable at room temperature, in that the crystals were unchanged over 2 days. As a general precaution, all reactions and experimental manipulations were carried out under nitrogen atmosphere, and solvents were degassed before use. The typical reaction yield was 95%.

Compound **1** crystallizes in the tetragonal space group $P4_2/mmm$ and its crystal structure is shown in Fig. 1.¹¹ The complex 3D perovskite structure can be described using three structural components: a) perovskite columns of corner-shared octahedra, $\text{CH}_3\text{NH}_3\text{SnI}_4$ ($4 = 4/2+2/1$); b) chains of *trans* corner-shared square pyramids, SnI_4 ($4 = 2/2+3/1$); c) isolated SnI_6 octahedra. The columns are normal perovskite units with CH_3NH_3 , Sn and I at the A-, B- and X-sites, respectively. The Sn–I bonding distances ($d_{\text{ave}} = 3.144$ Å) within the columns are similar to those observed in $\text{CH}_3\text{NH}_3\text{SnI}_3$ and their Sn(II) layered derivatives.^{6–10} The

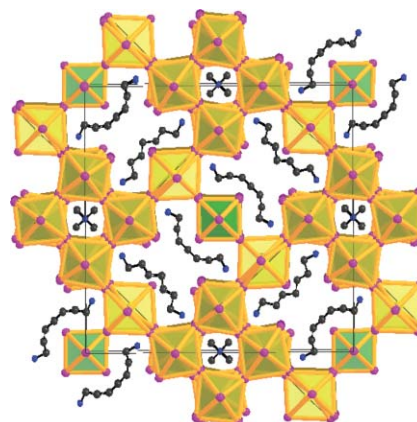


Fig. 1 A [001] view of the crystal structure of **1**. The $[\text{Sn}(\text{II})\text{I}_6]$ and $[\text{Sn}(\text{IV})\text{I}_6]$ octahedra are represented as dark-yellow and green polyhedra, respectively; $[\text{Sn}(\text{II})\text{I}_5]$ square pyramids are shown as light yellow pyramids; C and N are represented as black and blue spheres, respectively. The unit cell is outlined.

† Electronic supplementary information (ESI) available: crystallographic tables and diffuse reflectance spectrum for **1**. See <http://www.rsc.org/suppdata/cc/b4/b411322e/>

‡ This work was partially supported by the R. A. Welch Foundation, the Petroleum Research Fund and the NSF.

*aguloy@uh.edu

columns are further linked through their iodine-vertices, along the a - b plane, with the unshared basal vertices of the square pyramidal SnI_4 chains. The Sn–I distances ($d_{\text{ave}} = 3.11 \text{ \AA}$) in the SnI_5 square pyramids are also comparable to those in low-dimensional Sn(II)–I networks. The remaining A-sites are occupied by the terminal $-\text{NH}_3$ of the diamine cations, $\text{H}_3\text{N}(\text{CH}_2)_7\text{NH}_3$. The cations template cross-like cavities within the 3D perovskite network with vacancies occurring at the B- (Sn) and X- (I) sites. One type of empty B-sites, collinear with the Sn and the apical I of the square pyramids, are occupied by Sn which is further coordinated by six I atoms that do not coordinate to any other tin atom. However, two iodine atoms of the isolated octahedral SnI_6 units can be derived from a nominal octahedral coordination around the neighboring square pyramidal Sn. The square pyramidal SnI_5 and isolated SnI_6 units can be derived from a breathing mode distortion (contraction and elongation) of the Sn–I distances around adjacent SnI_6 octahedra with a concomitant formation of stereochemical lone pairs and isolation of the other SnI_6 octahedra. Inspection of the Sn–I distances within the different Sn–I polyhedra indicate the isolated SnI_6 octahedra exhibit significantly shorter Sn–I distances ($d_{\text{ave}} = 2.862(1) \text{ \AA}$) than those observed in other Sn(II) iodide perovskites. The observed Sn–I distances are comparable to Sn^{4+} –I distances in $\text{Cs}_2\text{Sn}^{4+}\text{I}_6$ (Sn–I (CN = 6): $2.864(1) \text{ \AA}$) and in tin(IV) iodide organometallic complexes (Sn–I (CN = 6): $2.78\text{--}82 \text{ \AA}$).¹² Assignment of the tetravalent oxidation state to the corresponding Sn atom yields the proper ionic charge balance: $[\text{H}_3\text{N}(\text{CH}_2)_7\text{NH}_3]^{2+}_8(\text{CH}_3\text{NH}_3)_2[\text{Sn}(\text{IV})\text{Sn}(\text{II})_{12}\text{I}_{46}]^{18-}$.

The defect structure of **1** from the perovskite can be traced to two B-site (Sn) vacancies in the structure. These are shown in Fig. 2. The first type (**A**) is surrounded by three iodines from neighboring SnI_6 octahedral units. Three other missing iodines ($2/2 + 1$) are associated with this vacancy resulting in a vacant “ SnI_2 ” unit. Similarly, the second vacancy (**B**) has 4 neighboring I from the neighboring Sn–I polyhedra ($2 \text{ SnI}_6 + 2 \text{ SnI}_5$). Two other missing iodines are part of a missing “ SnI_2 ” unit in vacancy **A**. The occurrence of Sn and I vacancies allows the alkyldiamine cations to occupy the A-sites of the perovskite framework, and the voids created by the vacancies are effectively compensated by the alkyl backbone of the cations. The ratio of **A** to **B** sites is 4 and the vacancies account for “ Sn_5I_8 ” in the idealized perovskite; i.e. “ $\text{A}_{18}\text{Sn}_{18}\text{I}_{54}$ ” – “ Sn_5I_8 ” = “ $\text{A}_{18}\text{Sn}_{13}\text{I}_{46}$ ”. The unit cell relationships also confirm the assignment, and a superstructure

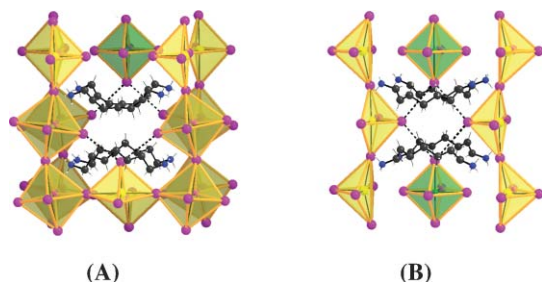


Fig. 2 The B-site vacancies, **A** and **B**, viewed along 001 and 110, respectively. Dashed lines indicate I coordination around each vacancy. The $[\text{Sn}(\text{II})\text{I}_6]$ and $[\text{Sn}(\text{IV})\text{I}_6]$ octahedra are shaded dark-yellow and green, respectively. The $[\text{Sn}(\text{II})\text{I}_5]$ square pyramids are shaded light-yellow. The C and N atoms are represented as black and blue spheres, respectively.

($l_{\text{cell}} \approx 3\sqrt{2}a_p \times 3\sqrt{2}a_p \times 2a_p$) of the perovskite cell (p) results from the ordered vacancies.

A crucial factor in the formation of the structure is that the distance between nearest neighbor A-sites ($\sim 6.3 \text{ \AA}$) and the *syn*-conformation length of the alkyl chain in the cation ($\sim 6.9 \text{ \AA}$) are essentially matched, and the $-\text{CH}_2\text{NH}_3$ ends of the diamine cations correspond to the CH_3NH_3 of the parent perovskite. Furthermore, incorporation of other diamine cations $\text{NH}_3(\text{CH}_2)_n\text{NH}_3$, $n \neq 7$ results in the expected non-defect layered perovskites.¹³ Thus, the critical templating role of the organic cation is convincingly exhibited in the novel structure. The end member of this new family of 3-D defect-perovskite structures, $[\text{NH}_3(\text{CH}_2)_7\text{NH}_3]_2\text{Sn}_3\text{I}_{10}$, has also been prepared.¹³

UV-Vis-NIR diffuse reflectance measurements indicated an optical band gap of 0.84 eV .¹⁴ The observed crystal structure and narrow-gap semiconducting behavior are consistent with a mixed-valent assignment, in accord with the Robin–Day model.¹⁵ This is surprising considering the cubic Sn(II) iodide perovskites are metallic and conducting due to delocalized Sn $5s^2$ electrons. Introducing ‘electronic holes’ in the form of Sn(IV) states apparently results in localization of the carriers (holes) at the $\text{Sn}(\text{IV})\text{I}_6$ octahedra. In addition, some Sn $5s$ states in the perovskite network are further localized at the $\text{Sn}(\text{II})\text{I}_5$ square pyramids as evidenced by the appearance of stereochemically active lone pairs. However, the remaining perovskite columns may still exhibit electronic character more associated with the conducting parent $\text{CH}_3\text{NH}_3\text{SnI}_3$. Interestingly, high-pressures may be needed in inducing the delocalization of the localized states (holes and lone-pairs), as in the mixed-valent Au(I/III) perovskites.¹⁶ More intriguing is that the hole concentration in **1** is 8% which closely approaches the hole concentrations in the superconducting perovskites.¹

Jun Guan, Zhongjia Tang and Arnold M. Guloy*

Department of Chemistry and the Center for Materials Chemistry, University of Houston, Houston, TX 77204-5003, USA. E-mail: aguloy@uh.edu

Notes and references

- (a) K. A. Muller and J. G. Bednorz, *Science*, 1987, **237**, 1113; (b) A. W. Sleight, *Science*, 1988, **242**, 1519; (c) R. J. Cava, *Science*, 1990, **247**, 656; (d) A. W. Sleight, *Acc. Chem. Res.*, 1995, **28**, 103.
- L. J. Tejuca and J. L. G. Fierro, Eds., *Properties and Applications of Perovskite Type Oxides*, Marcel Dekker, New York, 1993.
- C. N. R. Rao and B. Raveau, *Transition Metal Oxides*, VCH Publishers, Inc: Weinheim, Germany, 1995.
- (a) M. T. Anderson, J. T. Vaughey and K. R. Poeppelmeier, *Chem. Mater.*, 1993, **5**, 151; (b) D. M. Smyth, *Annu. Rev. Mater. Sci.*, 1985, **15**, 329.
- M. A. Pena and J. L. G. Fierro, *Chem. Rev.*, 2001, **101**, 1981.
- (a) D. B. Mitzi, *Prog. Inorg. Chem.*, 1999, **48**, 1; (b) G. C. Papavassiliou, *Prog. Solid State Chem.*, 1997, **25**, 125.
- (a) D. B. Mitzi, C. A. Field, W. T. A. Harrison and A. M. Guloy, *Nature*, 1994, **369**, 467; (b) D. B. Mitzi, S. Wang, C. A. Field, C. A. Chess and A. M. Guloy, *Science*, 1995, **267**, 1473.
- J. Guan, Z. Tang and A. M. Guloy, *Chem. Commun.*, 1999, 1833.
- D. B. Mitzi, *Inorg. Chem.*, 2000, **39**, 6107.
- (a) D. Z. Weber, *Z. Naturforsch., Teil B*, 1978, **33**, 862; (b) D. B. Mitzi, C. A. Field, Z. Schlesinger and R. B. Laibowitz, *J. Solid State Chem.*, 1995, **114**, 159.
- Crystal data: tetragonal, space group $P4_2/mnm$; $a = 26.9174(13) \text{ \AA}$, $c = 12.7329(9) \text{ \AA}$, $V = 9225.6(9) \text{ \AA}^3$, $Z = 2$; $\mu = 9.455 \text{ mm}^{-1}$; diffractometer, Siemens SMART; $T = 223 \text{ K}$; 47031 reflections measured, 4411 unique ($R_{\text{int}} = 0.0393$), 3523 reflections with $I/\sigma(I) > 2$, $R1 = 0.0527$, $wR2 = 0.1102$; $R1 = 0.0689$ and

-
- $wR2 = 0.1320$ (all data); Crystallographic Software: SHELXTL. Thermal parameters of non-hydrogen atoms were treated anisotropically. Idealized positions of H atoms were calculated (C–H = 0.96 Å, N–H = 0.90 Å). CCDC 246164. See <http://www.rsc.org/suppdata/cc/b4/b411322e/> for crystallographic data in .cif or other electronic format.
- 12 D. Tudela, A. J. Sanchez-Herencia, M. Diaz, R. Fernandez-Ruiz, N. Menendez and J. D. Tornero, *J. Chem. Soc., Dalton Trans.*, 1999, 4019.
 - 13 J. Guan, PhD Dissertation, University of Houston, 2001.
 - 14 (a) W. W. Wendlandt and H. G. Hecht, *Reflectance Spectroscopy*, Interscience Publishers, NY, 1966; (b) G. Kotiim, *Reflectance Spectroscopy*, Springer Verlag, New York, 1969.
 - 15 M. B. Robin and P. Day, *Adv. Inorg. Chem. Radiochem.*, 1967, **10**, 247.
 - 16 N. Kojima, M. Hasegawa, H. Kitagawa, T. Kikegawa and O. Shimomura, *J. Am. Chem. Soc.*, 1994, **116**, 11368.